

Short Communication

## Effect of $\beta$ -cyclodextrin as Organic Additive on Pulse Electrodeposition of Nanocrystalline Ni-W Coating

Qiangbin Yang<sup>1,2,3</sup>, Yi He<sup>1,\*</sup>, Yi Fan<sup>1,2,3</sup>, Yingqing Zhan<sup>2,3,\*</sup>, Ying Tang<sup>2,3</sup>

<sup>1</sup>State Key Lab of Oil and Gas Reservoir Geology and Exploitation (Southwest Petroleum University), Chengdu 610500, P. R. China

<sup>2</sup>Oil & Gas Field Applied Chemistry Key Laboratory of Sichuan Province (Southwest Petroleum University), Chengdu 610500, P. R. China

<sup>3</sup>School of Chemistry and Chemical Engineering, Southwest Petroleum University, Chengdu 610500, P. R. China

\*E-mail: [heyi007@163.com](mailto:heyi007@163.com), [327814719@qq.com](mailto:327814719@qq.com)

Received: 28 November 2015 / Accepted: 21 January 2016 / Published: 4 May 2016

---

Nanocrystalline nickel-tungsten (Ni-W) coatings was obtained by pulse electrodeposition in the plating bath with and without containing  $\beta$ -cyclodextrin ( $\beta$ -CD). The mirco-structure and morphologies of coatings were characterized by energy dispersive spectrometer (EDS), X-ray diffraction (XRD) and scanning electron microscopy (SEM). It was found that smaller grain size and more compact surface structure can be realized by introduction of  $\beta$ -CD, which had no influence on the compositions of the coating. More importantly, the coating had better anticorrosion and mechanical performance.

---

**Keywords:**  $\beta$ -cyclodextrin; Ni-W; nanocrystalline materials; corrosion; pulse electrodeposition.

### 1. INTRODUCTION

Nanocrystalline Ni-W was developed as one of the surface treatments due to high hardness, ductility, good wear resistance and corrosion resistance [1]. It was well accepted that electrodeposition is a versatile technique for producing nanocrystalline Ni-W. During the process of electrodeposition, the surface structure, morphologies and properties of coating can be regulated using small amounts of organic additives [2-7].

In general, the organic additives contain the following groups: sulfo, hydroxyl,  $>C=O$ ,  $>C=S$  or  $-C\equiv N$  [5-7]. They can adsorb on cathodic surface by their unsaturated molecular bonds, which would block the sites for Ni deposition and alternate deposition rate [4, 8, 9]. Recently, the widely studied organic additives in nickel plating baths were saccharin, 2-butyne-1,4-diol which contain aromatic

sulfonate and triple bonds, respectively [3, 4, 6, 10, 11]. The research results showed that addition of saccharin and/or 2-butyne-1, 4-diol can decrease the grain size of nickel plating. However, these organic additives can participated in the cathodic reaction, thus causing the consumption of additives during the process of electrodeposition [3, 12, 13]. For example, these research showed that the consumption rate of 2-butyne-1,4-diol and saccharin increased at agitation. To overcome these problems, it is necessary to introduce a new types of additives which will not be consumed during the process of electrodeposition.

Cyclodextrin (CD) with cyclic oligosaccharides is consisting of six to eight  $\alpha$ -1,4-D-glucose units, which were designated as  $\alpha$ ,  $\beta$ ,  $\gamma$ -CD, respectively [14]. Among these,  $\beta$ -CD has been widely used as the “supramolecular host” in the areas of biotechnology, pharmaceutical preparation, purification and polymer science because of its low cost and suitable cavity size for stabling and increasing the solubility of labile xenobiotics. More importantly, owing to the unique structure, the hydroxyl groups of on the edge of CD can bind with active metal through coordination bond [15, 16]. Therefore, it can absorb on the surface the cathode and effectively prevent the electrodeposition of Ni, which is beneficial for obtaining the small grain size of Ni-W and compact surface structure.

Herein, we report the  $\beta$ -CD as organic additives introduced in Ni-W electrodeposition bath. To our best of knowledge, the smaller grain size and more compact surface structure can be realized for Ni-W nanocrystalline coating, without affecting the compositions of the coating. The coating have good anticorrosion and mechanical properties.

## 2. EXPERIMENTAL

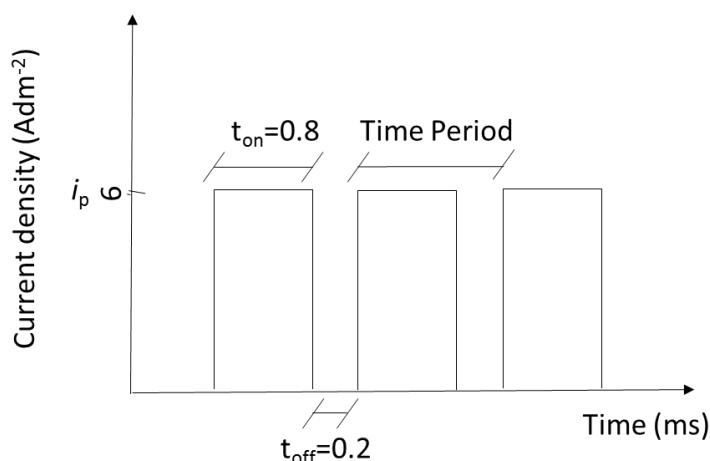


**Figure 1.** The used pulse-current waveform in the experiment

Ni-W nanocrystalline coatings were co-deposited by a pulse current electrodeposition from a citrate electrolyte, which was composed of 0.06 M NiSO<sub>4</sub>, 0.14 M Na<sub>2</sub>WO<sub>4</sub>, 0.15 M NaBr, 0.50 M Na<sub>3</sub>Cit, 0.50 M NH<sub>4</sub>Cl. Citric acid was employed to adjust the pH of 7.5. The 15 mm×30 mm×2 mm C45 carbon steel sheet was used as a cathode, and the graphite electrode was applied as an anode. Before the deposition of coating, the substrates were polished by using 800 and 1200 grit emery-paper

and ultrasonically cleaned with acetone and deionized water. Next, the substrates were activated with 1M sulfuric acid solution for 10 s at room temperature, followed by washing in distilled water and immersing into the plating bath. For all electroplating process, plating parameters were set as follows. As was shown in Fig. 1, the peak current density, frequency and duty cycle were set to be 6 A/dm<sup>2</sup>, 1000 Hz and 0.8, respectively. The plating bath was maintained at 70 °C and underwent a magnetic stirring for 1 hour at a constant speed of 200 rpm. Ni-W nanocrystalline coatings were obtained in the plating bath with and without containing 0.1 mM  $\beta$ -CD, which were named as C and C- $\beta$ , respectively.

Elemental compositions and surface morphologies of the coatings were characterized by energy dispersive spectrometry (EDS, INCA) and scanning electron microscopy (SEM, JSM-7500F), respectively. The grain structure and crystals orientation in film state was identified by X-ray diffraction (XRD, PANalytical X'Pert Pro diffractometer) with Cu *K* $\alpha$  radiation. Crystallite size was calculated by using the Scherrer equation.

Corrosion resistance were studied using electrochemical measurements by the conventional three-electrode cell, a platinum plate used as counter electrode, a saturated calomel electrode (SCE) as reference electrode and the samples as the working electrode. The exposed area of working electrode was 1cm<sup>2</sup>. The electrochemical impedance tests were conducted in the frequency range of 10-2-10<sup>5</sup> Hz with AC amplitude of 10 mV. The potentiodynamic polarization tests were taken with scanning from 250 mV vs SCE below OCP (open circuit potential) to 1000 mV vs SCE, with a scanning rate of 1 mVs<sup>-1</sup>. The parameters of corrosion current density (*i*<sub>corr</sub>) and corrosion potential (*E*<sub>corr</sub>) were calculated from the intersection of the anodic and cathodic by using the Tafel extrapolation way. Before all the tests, the working electrodes were immersed in the corrosive media for 1h to get a relatively steady OCP. The all measurements were carried out at room temperature and normally repeated at least three times under the same conditions to obtain reproducible data.

### 3. RESULTS AND DISCUSSION

The composition and morphology of Ni-W coatings were investigated by EDS and SEM, respectively. The result of EDS was presented in table 1. The element content were no obvious difference except carbon element. Since  $\beta$ -CD can adsorb on the cathode surface [16],  $\beta$ -CD may be incorporated into the coatings with Ni-W crystal growing during deposition, causing the increase of carbon content.

**Table 1.** The different element contents (wt.%) in the Ni-W nanocrystalline coating

Coatings	Element	Carbon	Oxygen	Nickel	Tungsten
C	Element	7.38	1.62	50.13	40.87
C- $\beta$	content (wt.%)	9.44	1.12	49.92	39.52

The effect of  $\beta$ -CD on crystal structure of the coatings was investigated by XRD, as shown in Fig. 2.

The patterns showed crystalline fcc structure of coatings with the predominant plane (1 1 1). With the addition of  $\beta$ -CD into the bath, the absorption intensity of the diffraction peak decreased, which indicated an decrease in the size of Ni-W grains as well as increased film stress [17, 18]. And the crystallite sizes of Ni-W coatings were calculated by Scherrer equation (1).

$$D = \frac{K\lambda}{B \cos \theta} \quad (1)$$

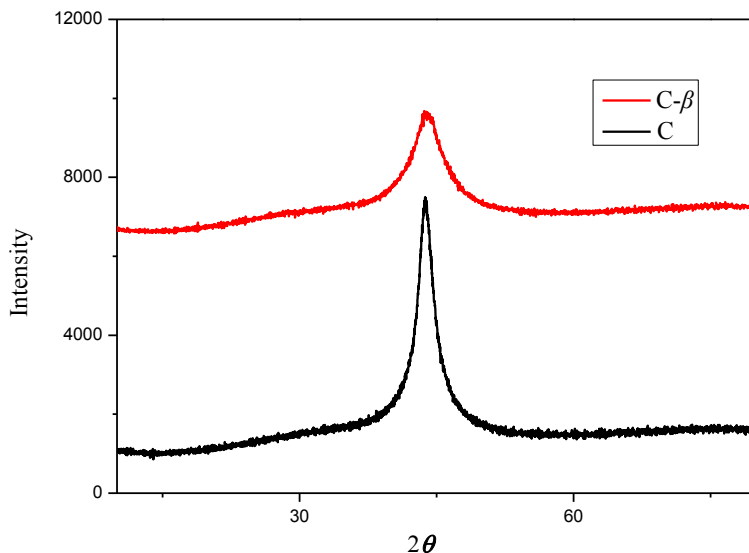


Figure 2. XRD patterns of the Ni-W nanocrystalline coating

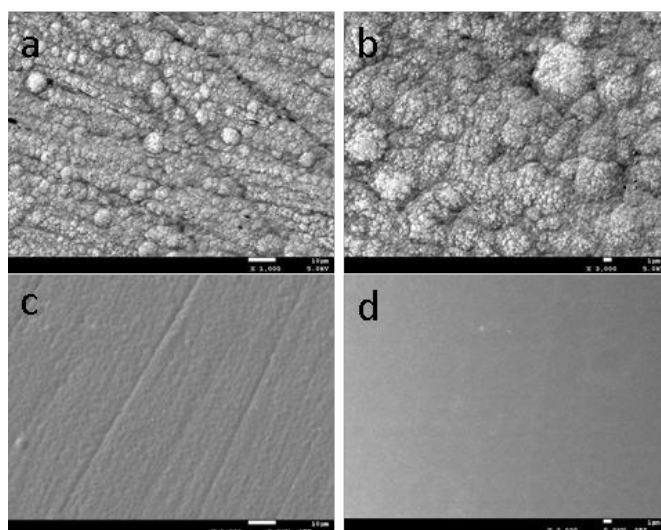


Figure 3. SEM images of the Ni-W nanocrystalline coating: (a) and (b) of C, (c) and (d) of C- $\beta$

Where  $D$  is the diameter of the crystal (nanometers),  $K$  is the shape factor (typical value is 0.89),  $\lambda$  is the incident radiation (1.5418 Å),  $B$  is the corrected peak width (radians) at half-maximum

intensity and  $\theta$  is Bragg's angle (degrees). The grain sizes of (1 1 1) plane of C and C- $\beta$ , were 21.0 and 4.6 nm, respectively. It indicated that the smaller nanocrystal size of Ni-W alloy can be gained by the introduction of  $\beta$ -CD in the plating bath. This is due to the fact that  $\beta$ -CD adsorbing on cathodic surface inhibit the growth of Ni-W crystalline grain.

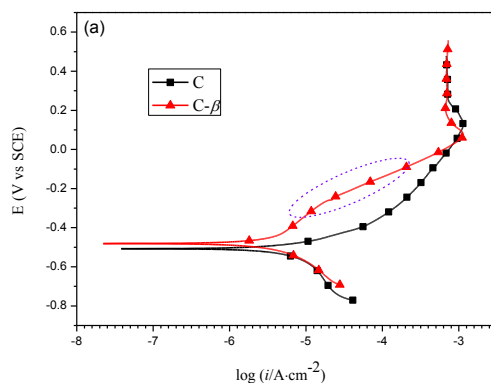
Typical surface morphology SEM images were shown in Fig. 3. Compared to the image of C (Fig. 2 a, b), the image of C- $\beta$  (Fig. 2c, d) exhibited a more compact and uniform surface structure, indicating that the introduction of  $\beta$ -CD can obtain smooth surface.

Corrosion resistance of the coatings were studied in 3.5 wt% NaCl solution. Potentiodynamic polarization curves were presented in Fig. 4(a). From the result of polarization, it was found that the curves of C- $\beta$  shifted to left in the higher potential of the anode Tafel curves (by circle), which is attributed to the formation of protection layer before occurred the passivation [19]. The  $i_{\text{corr}}$  and  $E_{\text{corr}}$  of the corresponding coatings were displayed in Table 2. It can be found the Tafel slope of the C- $\beta$  increased and  $i_{\text{corr}}$  significantly decreased and  $E_{\text{corr}}$  increased, which indicated C- $\beta$  had better anticorrosive performance. From the result of SEM and XRD, the surface of C- $\beta$  was more compact and the crystal size was smaller. The qualitative surface was easier to form a layer of protective oxide film before completely passivated. This indicated that the introduction of  $\beta$ -CD on the coating was conducive to corrosion resistance. The Nyquist plots and Bode plots of the coatings were presented in Fig. 4 (b) and (c). As the figure presented, those coatings exhibited semicircle at the high frequency, implying a capacitive loop. Besides, the C- $\beta$  had a different trend compared with the C at low frequency.

To explain electrochemical behavior of the coating surface, the C and C- $\beta$  were fitted by the equivalent circuit in the Fig. 4, respectively. In the Fig. 5 (a), a simple (RQ) parallel circuits was used to represent charge transfer resistance and the double layer capacitance, respectively. In the Fig. 4 (b), R and Q were representative the charge transfer resistance and the double layer capacitance in the high frequency, respectively.

**Table 2.** Electrochemical parameter for the coatings in the 3.5 wt% NaCl solution

The coating	$\beta_c$ (mV dec <sup>-1</sup> )	$\beta_a$ (mV dec <sup>-1</sup> )	$i_{\text{corr}}$ ( $\mu\text{A}/\text{cm}^2$ )	$E_{\text{corr}}$ vs SCE (V)
C	101.35	-565.32	8.16	-0.4827
C- $\beta$	294.87	-297.25	4.11	-0.4535



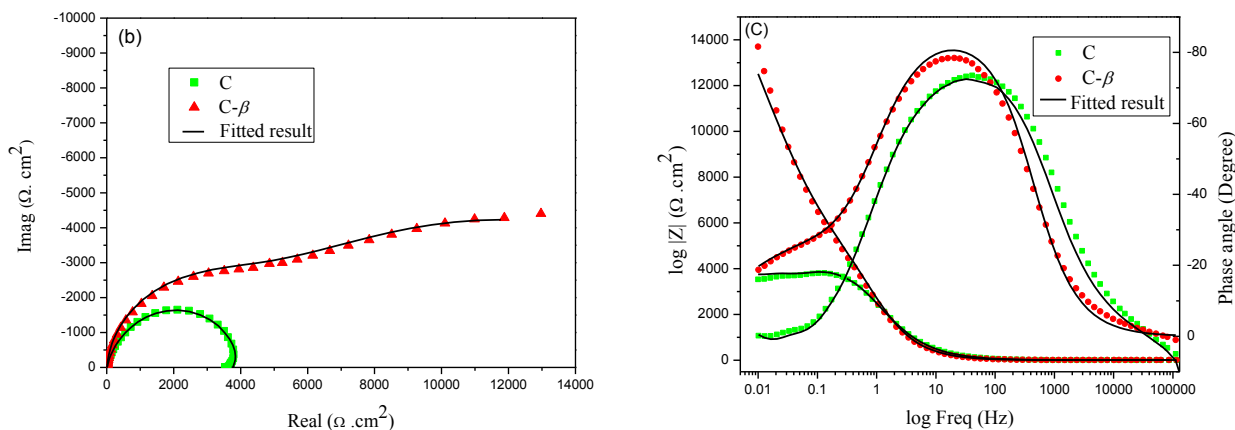


**Figure 4.** Electrochemical curves of Ni-W nanocrystalline coating in 3.5 wt% NaCl solution: (a) Polarization curves, (b) Nyquist diagram and (c) Bode plots

In the low frequency, the second ( $RQ$ ) parallel circuits was employed to represent the electrochemical activities of the passive film and the film/solution interface [20].  $R_f$  and  $Q_f$  were the film resistance and the film capacitance [21], or the resistance and capacitance of the space charge layer [22]. The fitted results were shown in Fig. 4, the experimental and fitted data were basically consistent in the Nyquist plots and Bode plots. And the impedance data obtained for the coatings were displayed at table 3. In the current research, Ni dissolved from the alloy matrix by galvanic action [23]. The coarse surface of C enlarged the reacted active sites, which caused the accelerated dissolution of Ni. The dissolving reaction would be inhibited on the compact surface, which also more easily formed oxide film than the coarse surface. The formed impedance membrane would result in the increase of impedance arc radius at the low frequency. The coating resistance ( $R_{cot}$ ) was used to represent corrosion resistance of the coatings. The coating resistance ( $R_{cot}$ ) indicated that the C- $\beta$  had the best corrosion resistance, revealing that the compact surface were conducive to corrosion resistance.

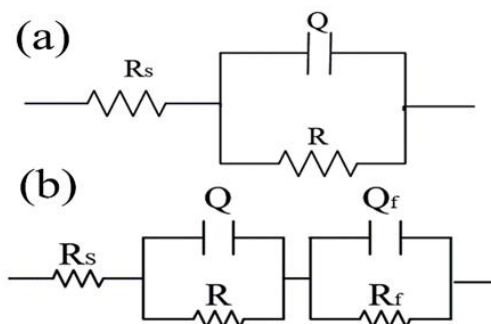


**Figure 4.** Equivalent circuit model for the Ni-W coatings

**Table 3.** Electrochemical parameters of equivalent circuit with experimental plots

The coatings	$R_s$ ( $\Omega \cdot \text{cm}^2$ )	$Q$ (F)	$R$ ( $\Omega \cdot \text{cm}^2$ )	$Q_f$ (F)	$R_f$ ( $\Omega \cdot \text{cm}^2$ )	$R_{\text{cot}}=R+R_f$
C	11.68	$7.7 \times 10^{-4}$	3856	-	-	3856
C- $\beta$	12.23	$5.6 \times 10^{-5}$	5234	$4.3 \times 10^{-4}$	12570	17804

The hardness of the coating was measured by loading of 300 g for 15 s. The micro-hardness for Ni-W alloy films increased from 263 to 288  $H_v$ . The mechanism of strengthening the polycrystalline metal and alloys was majorly influenced by grain refinement strengthening and dispersion hardening [24]. The C- $\beta$  had the small grain size, so micro-hardness value increased by grain refinement strengthening.

#### 4. CONCLUSION

Through introduction of  $\beta$ -CD in electrodeposition bath, the smaller grain size and more compact surface structure can be realized for Ni-W nanocrystalline coating, without affecting the compositions of the coating. Due to compact surface, C- $\beta$  was easier to form a layer of protected oxide film before completely passivated, the anticorrosion performance of Ni-W nanocrystalline coating was greatly improved. The C- $\beta$  had the small grain size increasing in micro-hardness value by grain refinement strengthening.

#### ACKNOWLEDGMENTS

This work was financial supported by the Applied Basic Research Project in Sichuan Province (2013JY0099) and the Majorly Cultivated Project of Sci-tech Achievements Transition from the Education Department in Sichuan Province (15CZ0005).

#### Reference

1. M.P.Q. Argañaraz, S.B. Ribotta, M.E. Folquer, L.M. Gassa, G. Benítez, M.E. Vela, R.C. Salvarezza, *Electrochimica Acta*, 56 (2011) 5898-5903.
2. T.C. Franklin, T.S. Narayanan, *Journal of the Electrochemical Society*, 143 (1996) 2759-2764.
3. D. Mockute, G. Bernotiene, *Surface and coatings technology*, 135 (2000) 42-47.
4. E.A. Pavlatou, M. Raptakis, N. Spyrellis, *Surface and Coatings Technology*, 201 (2007) 4571-4577.
5. T. Sakamoto, K. Azumi, H. Tachikawa, K. Iokibe, M. Seo, N. Uchida, Y. Kagaya, *Electrochimica Acta*, 55 (2010) 8570-8578.
6. E. Sezer, B. Ustamehmetoğlu, R. Katırcı, *Surface and Coatings Technology*, 213 (2012) 253-263.
7. A.M. Rashidi, A. Amadeh, *Surface and Coatings Technology*, 204 (2009) 353-358.
8. L. Oniciu, L. Mureşan, *Journal of Applied Electrochemistry*, 21 (1991) 565-574.
9. E.M. Oliveira, G.A. Finazzi, I.A. Carlos, *Surface and Coatings Technology*, 200 (2006) 5978-5985.
10. M. Holm, T. O'keefe, *Journal of applied electrochemistry*, 30 (2000) 1125-1132.
11. H.H. Abdel-Rahman, A.A. Harfoush, A.H.E. Moustafa, *Transactions of the IMF*, 91 (2013) 32-43.

12. D. Mockute, G. Bernotiene, R. Vilkaite, *Surface and Coatings Technology*, 160 (2002) 152-157.
13. J. Bocker, *Forschung und praxis, Proceuberwachung beim Galvanoformen*, vol. 69, in, Springer-Verlag, 1983.
14. H.-J. Buschmann, D. Knittel, E. Schollmeyer, *Journal of inclusion phenomena and macrocyclic chemistry*, 40 (2001) 169-172.
15. B. Fan, G. Wei, Z. Zhang, N. Qiao, *Corrosion Science*, 83 (2014) 75-85.
16. C. Zou, X. Yan, Y. Qin, M. Wang, Y. Liu, *Corrosion Science*, 85 (2014) 445-454.
17. S. Lee, M. Choi, S. Park, H. Jung, B. Yoo, *Electrochimica Acta*, 153 (2015) 225-231.
18. Y. Wu, D. Chang, D. Kim, S.-C. Kwon, *Surface and Coatings Technology*, 173 (2003) 259-264.
19. C. Cao, *Principles of Electrochemistry of Corrosion*, *Chemical industry press*, Beijing, (2008) 217-224.
20. H.-H. Ge, G.-D. Zhou, W.-Q. Wu, *Applied Surface Science*, 211 (2003) 321-334.
21. Q. Yin, G. Kelsall, D. Vaughan, N. Brandon, *Journal of the Electrochemical Society*, 148 (2001) A200-A208.
22. J. Jamnik, J. Maier, S. Pejovnik, *Electrochimica Acta*, 44 (1999) 4139-4145.
23. K.A. Kumar, G.P. Kalaignan, V. Muralidharan, *Ceramics International*, 39 (2013) 2827-2834.
24. A. Abdel Aal, *Materials Science and Engineering: A*, 474 (2008) 181-187.

© 2016 The Authors. Published by ESG ([www.electrochemsci.org](http://www.electrochemsci.org)). This article is an open access article distributed under the terms and conditions of the Creative Commons Attribution license (<http://creativecommons.org/licenses/by/4.0/>).